relation of S. J. Morbey [*Palaeontogr. Abh. B Palaeophytol.* **152**, 1 (1975)] is used here.

6. Diagnostic material of the ornithischian dinosaurs of the family Scelidosauridae is restricted to the English Lower Liassic [R. Hoffstetter, *Bull. Mus. Hist. Nat. Paris Ser. 2* **29**, 537 (1957)]. Theropod dinosaurs are represented by fragmentary remains of doubtful diagnostic value [M. Waldman, *Palaeontology* **17**, 325 (1974); A. F. Lapparent, *Sciences (Paris)* **51**, 1 (1967)]. The pterosaur families Dimorphodontidae and Rhamphorhynchidae occur throughout the early Mesozoic [A. S. Romer, *Vertebrate Paleontology* (Univ. of Chicago Press, Chicago, 1966)]. R. Zambelli [*Inst. Lombardo Rend. Sci. (B)* **107**, 27 (1973)] reports a dimorphodontid pterosaur from the Norian (Late Triassic) of Cene, Italy. Fragmentary pterosaurs are also reported from the Rhaetic of Germany [M. Schmidt, *Die Lebwelt Unserer Trias* (Hohenloh'sche Buchhandlung Ferdinand Rau, Oehringen, Germany, 1928)].
7. P. E. Olsen, in preparation.
8. B. Cornet, A. Traverse, N. G. McDonald, *Science* **182**, 1245 (1973); B. Cornet and A. Traverse, *Geosci. Man* **11**, 1 (1975).
9. R. L. Armstrong and J. Besancon, *Eclogae Geol. Helv.* **63**, 15 (1970).
10. R. S. Lull, *Bull. State Geol. Nat. Hist. Surv. Conn.* **18**, 1 (1953).
11. The form-family Grallatoridae consists of small to large theropod dinosaur footprints. Small forms (Grallatoridae "I" of Figs. 1 and 2) are found throughout the early Mesozoic, while large forms (Grallatoridae "II" of Figs. 1 and 2) are not common until the Rhaetic and Early Jurassic.
12. P. M. Galton, *J. Paleontol.* **45**, 781 (1971); *Postilla* **169**, 1 (1976).
13. H. G. Seeley, *Geol. Mag.* **50**, 1 (1898).
14. R. Dunay and A. Traverse, *Geosci. Man* **3**, 65 (1971); preliminary results of comparisons of Chinle-Dockum samples by B. Cornet (personal communication) (samples provided by S. Ash, Weber State College) with samples from zone 1 of the Newark Basin suggest correlation of both with the German Middle Keuper.
15. According to F. Peterson (personal communication), many geologists now consider the Rock Point member of the Wingate formation to be equivalent to the Church Rock member of the Chinle formation. The Rock Point member contains phytosaurs and should not be considered a part of the Glen Canyon group.
16. D. Lawler (personal communication) reports the discovery of a fabrosaurid(?) ornithischian dinosaur in the Kayenta formation of the Glen Canyon group.
17. S. P. Welles (University of California, Berkeley) has graciously supplied photographs of dinosaur footprints from the Glen Canyon group which show *Anchisauripus sillimani, Anchisauripus minusculus, Grallator* spp., *Anomoepus crassus*, and *Eubrontes* sp., all of which indicate a "Connecticut Valley" type of footprint assemblage. S. P. Welles [*Geol. Soc. Am. Bull.* **65**, 591 (1954)] has long maintained that the Glen Canyon group is Jurassic.
18. B. Cornet (personal communication) reports that a sample supplied by F. Peterson and C. E. Cristine Turner-Peterson from the Whitmore Point member of the Moenave formation of the Glen Canyon group indicates correlation with the Lower Liassic and zone 3 of the Newark Basin.
19. P. Ellenberger, *Paleovertebrata Mem. Extra.* (1974). Ellenberger has suggested elsewhere [in *Gondwana Stratigraphy, I.U.G.S. Symposium* (Unesco, Paris, 1967)] that the Upper Stormberg footprints indicate a correlation with the Liassic.
20. P. M. Galton and M. A. Cluver, *Ann. S. Afr. Mus.* **69**, 121 (1976).
21. A. S. Romer, in *International Symposium on Gondwana Stratigraphy and Paleontology, 3d.* (Australian National Press, Canberra, 1973), pp. 469–473.
22. A. S. Romer [*Brevoria* **395**, 1 (1972)] feels that A. D. Walker's [*Philos. Trans. R. Soc. London Ser. B* **257**, 816 (1970)] placement of the Middle Keuper *Saltoposuchus* in the Sphenosuchidae was not justified.
23. H. M. Anderson and J. M. Anderson, *Palaeontogr. Afr.* **13**, Suppl. (1970); K. A. Kermack, *Ann. Geol. Surv. Egypt* **4**, (1974).
24. K. A. Kermack, F. Mussett, H. W. Rigney, *J. Linn. Soc. London Zool.* **53**, 2 (1973); W. G. Kuhne, *The Liassic Therapsid Oligokyphus* [British Museum (Natural History), London, 1956]; P. L. Robinson, *J. Linn. Soc. London Zool.* **43**, 291 (1956).
25. C. B. Cox, *in The Fossil Record* (Geological Society of London, London, 1967), pp. 77–89; P. L. Robinson, *Palaeontology* **14**, 131 (1971).
26. This is corroborated by F. J. Fitch and J. A. Miller's [*Bull. Volcanol.* **35**, 1 (1971)] radiometric dates of 181 to 165 million years B.P. from the Drakensberg Volcanics overlying and interbedded with the Cave Sandstone of the Stormberg group, a range which is younger than the volcanics in the basal part of zone 3 of the Newark Basin of the Newark supergroup and is certainly Liassic.
27. W. J. Arkell, *Jurassic Geology of the World* (Oliver & Boyd, London, 1956); A. L. Du Toit, *Geology of South Africa* (Oliver & Boyd, Edinburgh, 1954).
28. E. H. Colbert, *The Age of Reptiles* (Norton, New York, 1965); A. S. Romer, *Vertebrate Paleontology* (Univ. of Chicago Press, Chicago, 1966).
29. F. B. Van Houten, *Bull. Am. Assoc. Pet. Geol.* **61**, 79 (1977).
30. Coeluridae is used in a broad sense to include the Procompsognathidae because separation of these two families is mostly based on the supposed restriction of the Procompsognathidae to the Triassic.
31. The type maxilla of *Teratosaurus* from the Stubensandstein (Middle Keuper) may belong to a megalosaur, and M. Waldman [*Palaeontology* **17**, 325 (1974)] reports that a jaw from the English Rhaetic is indistinguishable from *Megalosaurus*.
32. Some of the larger prosauropod remains from the Middle Keuper are probably melanorosaurid, and *Avalonia* [see (*13*)] from the English Rhaetic certainly is [A. J. Charig, J. Attridge, A. W. Crompton, *Proc. Linn. Soc. London* **176**, 197 (1965)].
33. Data for Rhaetic distribution of footprints are from A. F. deLapparent and C. Montetat [*Mem. Soc. Geol. Fr.* **46**, 1 (1967)] and data for the Liassic record are from P. Ellenberger [*C. R. Acad. Sci.* **260**, 5856 (1965)] and L. Thaler [*C. R. Somm. Sceances Soc. Geol. Fr.* (1962), p. 190].
34. The concurrence of *Patinasporites* and *Ovalipollis* indicate Late Triassic, and a preponderance of *Corollina* (> 90 percent) is typical for the Early Jurassic (B. Cornet, personal communication).
35. Parts A to D of Fig. 2 are from the Pratt Museum of Amherst College, Amherst, Mass., Nos. 16/5, 45/1, 16/1, and 9/14, respectively; Fig. 2E is adapted from D. Baird, *Bull. Mus. Comp. Zool. Harv. Univ.* **111**, 163 (1954); Fig. 2F is adapted from D. Baird, *ibid.* **117**, 449 (1957); Fig. 2G is from Yale Peabody Museum No. 7703; Fig. 2H is from a series of trackways on a slab at the New York State Museum No. V-86.
36. Middle Jurassic faunas are very poorly known, and it is possible that groups which are shown to become extinct (Fig. 4) in the Early Jurassic actually survived into the Middle Jurassic [E. H. Colbert, *The Age of Reptiles* (Norton, New York, 1965)]. The ranges of the Fabrosauridae and the Heterodontosauridae are drawn without the inclusion of several undescribed Newark hypsilophodontid-like forms, or *Pisanosaurus*, or *Tatisaurus*, because of their extremely uncertain taxonomic relationships [P. M. Galton, *Nature (London)* **239**, 464 (1972)].
37. We thank D. Baird, B. Cornet, J. H. Ostrom, F. Peterson, and S. Rachootin for their assistance. This work was supported by grant BM 574-07759 from the National Science Foundation to K. S. Thomson.

25 February 1977; revised 6 May 1977

Lunar Surface Chemistry: A New Imaging Technique

Abstract. *Detailed chemical maps of the lunar surface have been constructed by applying a new weighted-filter imaging technique to Apollo 15 and Apollo 16 x-ray fluorescence data. The data quality improvement is amply demonstrated by (i) modes in the frequency distribution, representing highland and mare soil suites, which are not evident before data filtering and (ii) numerous examples of chemical variations which are correlated with small-scale (about 15 kilometer) lunar topographic features.*

The Apollo 15 and Apollo 16 missions to the moon carried an x-ray fluorescence spectrometer, which measured from orbit the aluminum, silicon, and magnesium concentrations in surface soils, using the x-ray emission from the sun as the exciting source (*1, 2*). The primary objective of the experiment was to map the geochemistry of the areas overflown in terms of these major rock-forming elements. Knowledge of the composition and distribution of chemical components is fundamental to a reconstruction of the evolution of the moon, including its origin, accretion, chemical differentiation into rock types, and physical processes which have modified the lunar crust.

The elemental measurements are expressed as intensity ratios (Al/Si, Mg/Si, and Mg/Al) in order to minimize nonchemical effects on the measured signal, such as those caused by differences in sun-moon-spacecraft geometry, shifts in the solar spectrum, and particle size variations on the lunar surface.

The important relationship between orbital x-ray intensity ratios and "ground truth" (returned sample) analyses is based on the fact that the characteristic secondary x-ray intensity is directly related to the element's concentration in surface soils. The conversion factors for intensity to concentration ratios have been determined by correlating orbital data with chemical analyses of returned soils from the Apollo and Soviet Luna missions. This critical link is the basis for extending detailed chemical information from a few specific landing sites to broad areas of the moon traversed by the Apollo 15 and Apollo 16 spacecrafts.

A new technique has recently been developed to convert the digital information from Apollo orbital x-ray data to a color image of chemical variations on the lunar surface. The image shown in Fig. 1 is the first detailed color representation of chemical variations constructed en-

Fig. 1. Map displaying chemical variations across the lunar surface based on data from the Apollo 15 and Apollo 16 orbital x-ray fluorescence experiments. The colors represent different values of Al/Si concentration ratios.

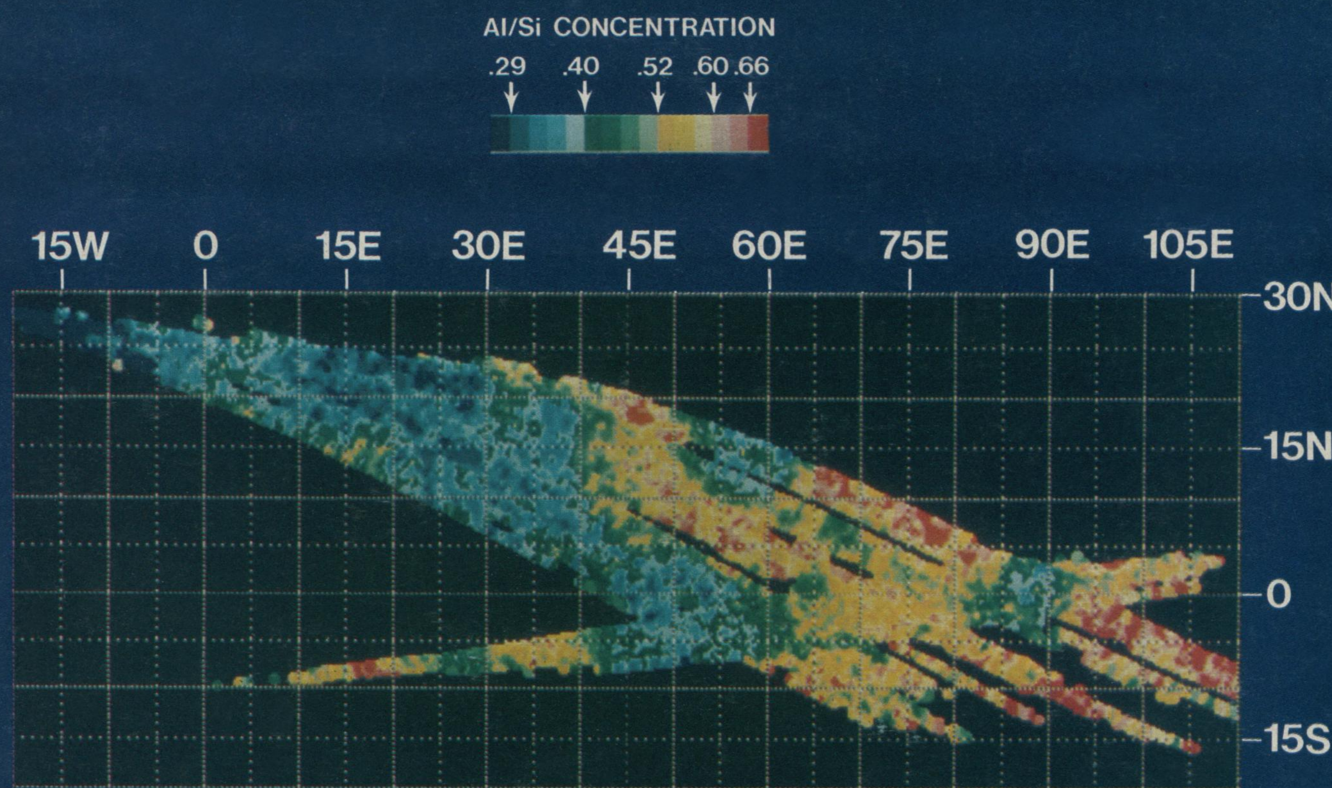
Al/Si CONCENTRATION
.29 .40 .52 .60 .66
15W 0 15E 30E 45E 60E 75E 90E 105E
30N
15N
0
15S

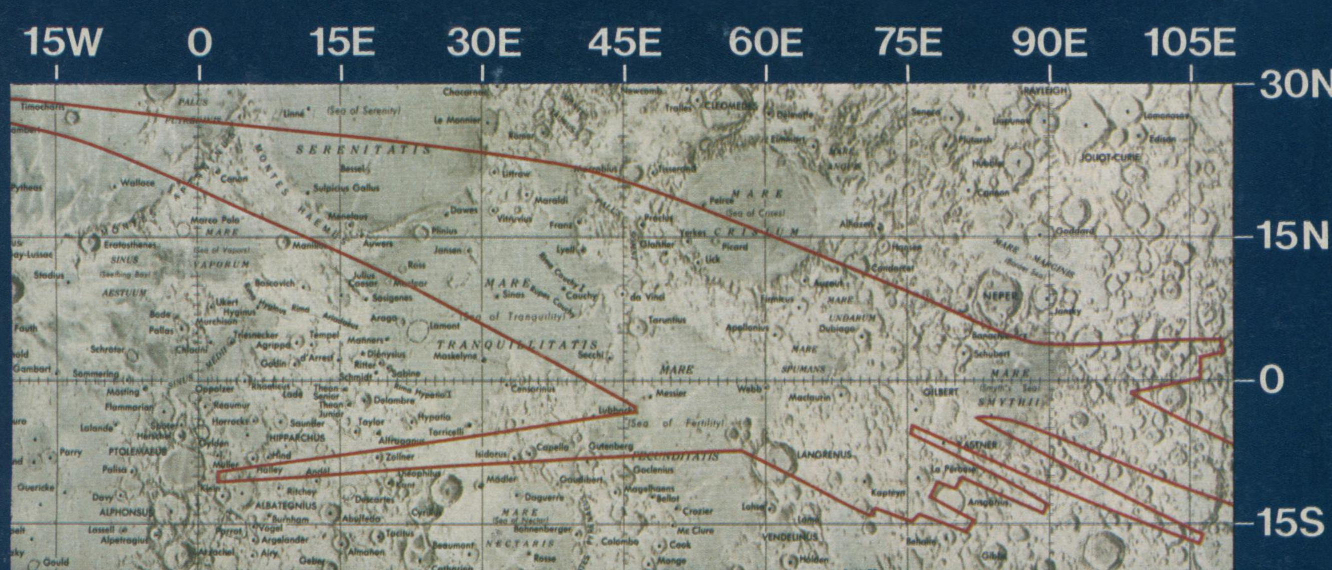
15W 0 15E 30E 45E 60E 75E 90E 105E
30N
15N
0
15S

tirely from 9000 Al/Si data points from the Apollo x-ray data. The application of this technique to x-ray data serves as a prototype for standardizing numerous lunar geochemical and geophysical data sets for correlation purposes.

The spatial resolution of the Al/Si data shown on this image has been improved by more than a factor of 40 over that of a previous color map (*3*) produced by averaging the data within large topographic regions. The image displays a surprising amount of chemical detail, which can be correlated with lunar topographic features with dimensions on the order of 15 km. Mare material and highland material can be clearly distinguished, yet each regime shows a range of chemical compositions. Small lunar features such as flooded craters, ejecta blankets, and remnants of multiple ring systems concentric to basins can be identified on the basis of chemistry alone.

Integration of these numerous intensity ratios into a detailed geochemical map has been successful because of the data reduction methods and much improved array processing techniques. Preparation of the data base before array processing involved three steps. (i) To maintain consistency in mapping the geographic location and areal extent of chemical changes measured, values were excluded if the spacecraft attitude caused the center of the field of view to veer more than 10° from the subspacecraft point. (ii) The mean level of Al/Si values for each orbit was adjusted to compensate for interorbit variations due to solar spectral changes during the 2-hour time lapse between orbits. It has been established that a more energetic solar spectrum causes enhanced excitation of the Si radiation relative to that of Al (*1*). These adjustments, involving factors of about 7 percent, did not distort ratio variations along the individual orbits and maintained the mean intensity ratio for the mission as a whole. (iii) From an analysis of more than 750 data points within the region of mission overlap, a factor of 0.92 was determined for the normalization of the Apollo 16 data to the Apollo 15 data in order to compensate for the slightly different solar conditions for the missions.

The versatile array processing techniques developed by the U.S. Geological Survey (USGS) in Flagstaff, Arizona, are especially suitable for Al/Si data. Because of the unique character of the USGS system, x-ray image processing, which requires arithmetic precision, could be done in 32-bit floating-point arithmetic. Most important, the imaging process is designed to extract chemical detail which is concealed by the following characteristics of the x-ray data points. (i) Intensity measurements, recorded over a period of 8 seconds, correspond to points along the ground track which are about 12.5 km apart, whereas the instantaneous field of view is about 110 km in diameter. Therefore, eight to nine consecutive data points have overlapping signals. (ii) Interorbit distances between data points vary as a function of trajectory. (iii) Statistical errors vary from point to point. (iv) Signal intensity decreases with distance from the center of the field of view.

To address these problems, data points have been integrated by a series of increasingly large data filters which simulate the radial response of the spectrometer's field of view. The smallest filter represents a 7.5-km^2 area of the lunar surface. The next three filters in the series are concentric about the smallest filter and increase in size up to 52.5 km on an edge. Each filter incorporates data points weighted on the basis of statistical error. Furthermore, each Al/Si value calculated for the four filters is weighted so that the smaller the filter, representing an area closer to the center point, the more influential the value. When this set of concentric filters is moved along the lunar surface in 7.5-km steps, each pixel unit on the image represents the best possible balance between statistical significance and spatial resolution. The resulting image of the Al/Si concentration ratio on the lunar surface is seen in Fig. 1.

The dramatic effect of the weighted filtering can be seen in a comparison of the frequency distributions for the same Al/Si measurements before and after the filtering procedure (Fig. 2). Most significant is the fact that the amorphous profile of the unfiltered data breaks into two clearly distinct distributions of Al/Si values. These modes are obscured in the unfiltered data because of random fluctuations due to the large errors associated with single 8-second Al/Si data points. The amplitude of the two modes applies only to the area overflown and is not an indication of the relative amounts of the two compositional groupings for the lunar surface as a whole. A range of Al/Si values from those of mare basalt to those of highland material has been observed in previous analyses (*1–4*). However, this bimodal distribution is the first clear demonstration that orbital x-ray data can discriminate between the two most com-

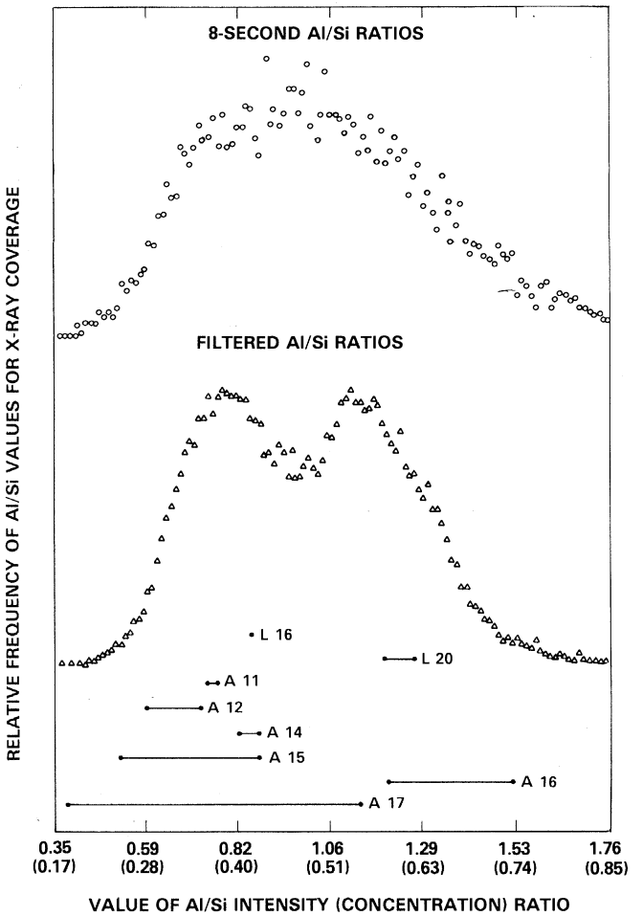

Fig. 2. Frequency distributions for Al/Si measurements before and after the weighted filtering procedure. Horizontal bars show Al/Si ranges based on chemical analyses of soils from all Apollo (*A*) and Luna (*L*) missions.

mon soil suites, mare and highland, known to exist on the moon.

One important aspect of this x-ray frequency distribution is that the chemistry of returned samples may be placed in the context of the broader orbital coverage of the lunar surface. The ranges of Al/Si concentration ratios based on chemical analyses of soils from all Apollo and Luna missions are indicated by horizontal bars in Fig. 2. The frequency of occurrence for the soil ranges shown indicates the degree to which that material is representative of the areas overflown by the Apollo spacecrafts.

It is of interest to note that within the quality of the measurements there appear to be compositional continua about both highland and mare modes. There does not appear to be any significant amount of material within the mapped area having Al/Si values lower than those of the Apollo 17 black and orange soils.

The following geochemical features seen on the image are useful clues to lunar evolutionary processes.

1) The chemical composition of the maria becomes more aluminous from west to east.

2) Nonmare areas become increasingly Al-rich from west to east, with the exception of the Descartes area (17°E; 8°S), which has Al/Si values as high as those of highland areas east of 40°E.

3) Considerable variation in Al/Si values within highland areas demonstrates that the lunar crust is not homogeneous.

4) It is apparent from variations in Al/Si that the Smythii basin (80°E to 90°E; 5°S to 5°N) is only partially flooded with basalt.

5) A concentric pattern of Al/Si variations around the Crisium basin (50°E to 65°E; 10°N to 20°N) suggests a chemical correlation with the topographic expression of a multiple ring system. This pattern may represent disruption of crustal stratigraphy or mare basalt flooding in the topographic lows between the rings. A more detailed analysis is required to resolve this question.

6) Low Al/Si values immediately to the west of and within the Firmicus crater (63°E; 8°N) and within the Miraldi crater (35°E; 19°N) support photogeologic evidence that mare basalts have flooded the floors of these craters. Identification of these basalt-filled highland craters, which have distinct Al/Si signatures, provides information about the volumes and distribution patterns of mare basalt flows on the lunar surface.

7) The postmare crater, Langrenus (61°E; 8°S), exhibits a traceable high-Al/Si ejecta blanket extending west into Mare Fecunditatis. This ejecta is detectable from x-ray data because the highland-type material displaced contrasts chemically with the adjacent mare surface. The extent of primary ejecta in proportion to the crater size is significant for studies of crater mechanics and for volume estimates of material excavated by meteorite impact.

8) The craters Capella (35°E; 7.5°S), Apollonius A (57°E; 5°N), and Taruntius (46.5°E; 5.5°N) have higher Al/Si values than the adjacent intermare areas, suggesting that the impacts exposed a lower stratigraphic horizon of higher Al/Si material.

9) The postmare craters Plinius (24°E; 15.5°N) and Ross (22°E; 12°N) appear to have penetrated thin mare basalts and excavated material from the more aluminous basin floor zone. The nature of subsurface material may be observed through the "window" of impact craters. The depths of craters which sample basin floor material help to define submare basin morphology and constrain estimates of the maximum depth of mare basalt flows.

10) A streak of lower Al/Si values crosses both Mare Fecunditatis and highland areas from southwest to northeast (intersecting coordinates 59°E; 3°N and 54°E; 2°S). This streak is parallel to and only slightly offset from a mapped ray radial to the Tycho event.

Finally, it is worth noting that the area mapped to date from x-ray data constitutes less than 10 percent of the lunar surface. For complete interpretation of these data and for full exploitation of the Apollo and Luna returned lunar sample information, it is of utmost importance that x-ray data be obtained over the whole moon so that the full range of surface soil compositions may be characterized and mapped in detail. The opportunity to accomplish this important goal is readily available in the projected Lunar Polar Orbiter mission, with its global mapping capability.

CONSTANCE G. ANDRE
Chemistry Department, University of Maryland, College Park 20742
MICHAEL J. BIELEFELD
Computer Sciences Corporation, Silver Spring, Maryland 20910
ERIC ELIASON
LAURENCE A. SODERBLOM
U.S. Geological Survey, Flagstaff, Arizona 86001
ISIDORE ADLER
Chemistry Department, University of Maryland, College Park 20742
JOHN A. PHILPOTTS
Goddard Space Flight Center, Greenbelt, Maryland 20771

References and Notes

1. I. Adler, J. Gerard, J. Trombka, R. Schmadebeck, P. Lowman, H. Blodget, L. Yin, E. Eller, R. Lamothe, P. Gorenstein, P. Bjorkholm, B. Harris, H. Gursky, in *Proceedings of the Third Lunar Science Conference*, D. Criswell, Ed. (MIT Press, Cambridge, Mass., 1972), vol. 3, pp. 2157–2178.
2. I. Adler *et al.*, *Science* **177**, 256 (1972).
3. I. Adler, J. Trombka, R. Schmadebeck, P. Lowman, H. Blodget, L. Yin, E. Eller, M. Podwysocki, J. R. Weidner, A. L. Bickel, R. K. L. Lum, in *Proceedings of the Fourth Lunar Science Conference*, W. Gose, Ed. (Pergamon, Elmsford, N.Y., 1973), vol. 1, frontispiece.
4. M. H. Podwysocki, J. R. Weidner, C. G. Andre, A. L. Bickel, R. S. Lum, I. Adler, J. E. Trombka, in *Proceedings of the Fifth Lunar Science Conference*, W. Gose, Ed. (Pergamon, Elmsford, N.Y., 1974), vol. 3, pp. 3017–3024.
5. We gratefully acknowledge use of the imaging facilities of Code 930 of Goddard Space Flight Center. Supported by NASA grant NGR-21-002-368.

22 June 1977; revised 19 July 1977

Nucleon Stability: A Geochemical Test Independent of Decay Mode

Abstract. *By analyzing published geochemical data on xenon isotopes measured in a 2.46 × 10^9-year-old telluride ore, a lower limit of 1.6 × 10^{25} years has been obtained for the mean lifetime of the nucleons in the tellurium-130 nucleus. This result is insensitive to the particular mode by which the nucleons decay and therefore provides a rigorous limit on possible baryon number nonconservation. The new limit is about two orders of magnitude better than the previous rigorous limit on nucleon stability.*

The law of baryon conservation, first proposed by Stückelberg (*1*) and by Wigner (*2*), has recently received renewed attention because of the prediction by several unified gauge theories (*3*) of the weak, electromagnetic, and strong interactions that this law may not be exact (*4*). From an experimental point of view, the most sensitive tests of baryon conservation are provided by searches for decays of nucleons (*5*), since such decays, at least into known particles, cannot occur without violating the law of baryon conservation. Estimates of the nucleon lifetime provided by the various unified gauge theories (*3*) range from 10^{27} to 10^{35} years.

A limit of 2 × 10^{30} years has been